IEEE Transactions on Vehicular Technology, Volume 60, Number 2, February 2011, Pages 390-405

FEASIBILITY OF HIGH FREQUENCY AC POWER FOR MOTOR AUXILIARY LOADS IN VEHICLES

CIPRIAN ANTALOAE, JAMES MARCO, NICHOLAS D VAUGHAN

J.MARCO@CRANFIELD.AC.UK

ABSTRACT

This paper presents a feasibility study into the application of a 100V, 50kHz high frequency alternating current (HFAC) network for powering automotive electrical auxiliaries. The study is focused on motor-actuated loads, and is divided into two sections. First, the investigation indicates the benefits of replacing low-torque DC motors with lighter and more efficient 400Hz AC machines for applications such as electric fans, fuel pumps or blower motors. A comparative examination of commercially available machines indicates space and weight reduction of more than 60%, and efficiency savings between 25% and 100% are possible. Second, the inquiry evaluates the viability of replacing existing DC/AC inverters with HFAC/AC converters for high-torque AC machines as employed for example in the electric power assisted steering (EPAS) or the heating, ventilation and air conditioning (HVAC) systems. Based on experimental and simulation results for a column-assist EPAS application, employing a three-phase permanent magnet synchronous motor, this study shows that a HFAC drive is expected to reduce the voltage harmonic content below 50kHz by at least 10% compared to the DC/AC inverter. However, the disadvantages of the former drive make it less attractive than the existing DC/AC circuit. Specifically, the EPAS motor torque ripple is expected to be approximately 2% higher compared to the DC counterpart drive. Further drawbacks of the HFAC/AC drive include high MOSFET conduction losses, higher voltage harmonics above 50kHz and complex control requirements of the inverter. Conclusively, significant HFAC advantages for motor loads can be attributed only to machines with a nominal torque capability that is limited to 2Nm. However, given the number of such devices within a typical vehicle, this translates into a possible vehicle mass saving of 30kg and a potential reduction in fuel consumption by 0.8L/100km.

KEYWORDS

High Frequency Alternating Current, Electric Power Assisted Steering, Space Saving, Mass Reduction, Distributed Electrical Architecture.

TERMS AND ABBREVIATIONS

DC - Direct Current
EPAS - Electric Power Assisted Steering
EMI - Electromagnetic Interference
HFAC - High Frequency Alternating Current
HVAC - Heating, Ventilation and Air-Conditioning
LED - Light Emitting Diode
OEM - Original Equipment Manufacturer
PDM - Pulse Density Modulation
PM - Permanent Magnet
PMSM - Permanent Magnet Synchronous Motor
PWM - Pulse Width Modulation
SV - Space Vector
THD - Total Harmonic Distortion
VVT - Variable Valve Timing
ZVS - Zero Voltage Switching
ZCS - Zero Current Switching

I. INTRODUCTION

The increased levels of vehicle electrification and the widespread deployment of electronic control systems are widely seen as the enabling technology for a number of the safety, driver assistance, infotainment and powertrain features of new vehicles (Lukic and Emadi, 2002, Lukic and Emadi, 2003, Emadi et al., 2004). Recent studies, such as (Line et al., 2008, Jonasson and Roos, 2008, Uchida et al., 2007, Eki et al., 2007), have highlighted the trend associated with the transition of the vehicle from being primarily a mechanical system to a mechatronic one, containing a number of higher power and in some cases safety-critical and *by-wire* systems. The problem with this trend is that the power demand of state-of-the-art applications is expected to exceed the capability of the current 14V DC system. Although an alternative 42V DC *PowerNet* has been proposed by the SAE Dual/Higher Voltage Committee in the early 1990s to solve this issue, technical hurdles such as electric arcs, connector corrosion problems and bus-to-bus faults have yet to be overcome (Keim, 2004, Caliskan, 2000, Doublet et al., 2004). A high frequency AC (HFAC) power bus is potentially the solution due to its feasibility for applications with a cumulative power rating of 4kW, as detailed in the study by Antaloae et al. (2010a). Also, the reliability problems related to high voltage connectors can be eliminated since the HFAC system utilises magnetic and galvanically-isolated connectors.

However, the automotive industry is characterised by high levels of competition coupled with continuous consumer pressure for ever increasing levels of vehicle performance, fuel economy and price reduction. The long-term sustainability of HFAC technology will therefore largely depend on the ability of the industry to integrate HFAC systems in a manner that maximises both the performance and environmental attributes of the vehicle, while concurrently helping to shorten development times and production costs.

The motivation for researching the application of HFAC as a possible replacement for the conventional DC in-vehicle power distribution network is summarised below:

First, HFAC cables are a comparatively lightweight and efficient. A detailed case study contained within (Antaloae et al., 2010b) highlights a potential copper weight saving of 70% and 30% for a 50kHz, 100V AC bus when compared to 14V and 42V DC systems, respectively. Also, based on the same comparison, the study indicates an increase in power distribution efficiency by 90% and 80%, respectively. The high operating frequency of the network also facilitates the design of more compact circuit elements such as capacitors, inductors and transformers. In addition, smaller, lightweight and more efficient electrical motors operating at 400Hz can be easily interfaced from a HFAC bus using frequency converters. As a result, such machines may potentially replace existing low torque DC motors in a number of vehicle applications. DC machine technology is known to integrate permanent magnets, which add considerably to their weight

in comparison to AC machines (Masrur et al., 1998a).

Second, the HFAC network inherently enables a more distributed topology with power conversion undertaken locally at the point of use. As discussed in (Kassakian et al., 1996), this architecture will in turn facilitate easier technology integration and fault diagnosis. Both activities are widely reported as being challenging and resource-intensive, especially when dealing with conventional DC systems in which the network may typically contain up to 600 sub-modules and connectors, 1500 wires and up to 2000 terminals (Honeywill, 2007).

The third motivation relates to the fact that simultaneous power regulation can be achieved for all the loads connected to the HFAC bus, unlike within some 42V/14V DC power networks where only one of the buses can be regulated at any given time (e.g. dual-stator alternator (Caliskan, 2000), dual-reference alternator or transformer/rectifier power net (Smith, 1991)). It is essential for new network topologies to meet the demand for different voltage levels concomitantly, since it is expected that loads will require voltages ranging from 5V for instruments and electronic control units, to 14V for the majority of the existing loads in vehicles, and a higher voltage for modern loads that require more than 2kW such as the engine electromechanical valves or active suspension systems (Rajashekara, 2003). In addition, electrical systems based on current at frequencies above 10kHz are known to represent a less hazardous working environment for humans than equivalent DC networks or those employing lower-frequency AC current (Patel, 2005).

The transformers employed within a HFAC architecture not only have a typical power conversion efficiency above 95% (Wong, 2004) but also provide galvanic isolation for the different sub-systems connected to the bus. Furthermore, any output voltage or current level is easily obtainable by appropriately choosing the turns-ratio of the transformer windings. This in turn, facilitates the potential optimisation of the actuator design in-line with a specific voltage level rather than the generic 14V supply.

The potential advantages highlighted above associated with the use of HFAC have motivated a number research institutions and original equipment manufacturers (OEMs) to investigate the application of AC for in-vehicle power distribution. The voltage and frequency levels under consideration have typically ranged from 48V to 440V and from 400Hz to 25kHz, using either a square-wave or sinusoidal voltage waveform. The research conducted by Kokes (1997) primarily focuses on the feasibility and performance of a 4kW DC/HFAC inverter and power distribution based on a square-wave voltage at 80V, 25kHz. The same frequency was considered by Kassakian et al. (1996) for a 48V auxiliary electrical system, where loads are interfaced by local power converters at different locations in the vehicle. The only examination of HFAC for power distribution within a hybrid electric vehicle (HEV) was undertaken by Bose

et al. (1996), which focused on the general description of a 20kHz, 440V system.

While the studies highlighted above share the same generic concept of replacing DC with HFAC, the focus is directed to either an in-depth analysis of the power generation sub-system (Kokes, 1997) or towards a general description of the HFAC system (Bose et al., 1996, Kassakian et al., 1996) with little detail or only qualitative evidence being provided as to the benefits of HFAC for auxiliary electrical loads.

Within the context of this study, the most pertinent publications are by Masrur et al. (1998a, 1998b), which present an analysis of the tradeoffs associated with replacing the auxiliary DC system within vehicles with an alternative 400Hz AC system, using either a single-phase or three-phase voltage supply. In addition to a qualitative system-level examination, the study by Masrur et al. (1998a, 1998b) cites the two main advantages for 400Hz AC as being:

- firstly, the use of optimised three-phase AC machines which can be up to 40% smaller than comparable DC motors, and
- secondly, a financial cost saving for both three-phase and single-phase motors with a power factor higher than 0.737 and 0.956, respectively. In particular, a normalised cost saving of up to 0.7 was noted for three-phase 400Hz machines with a power and torque rating of 122W and 90Ncm, respectively, in comparison to DC motors.

What differentiates the research presented within this paper is that it provides a comprehensive and timely account of the benefits of HFAC power for vehicle auxiliaries based on motor actuators. The qualitative benefits of 400Hz AC motors as presented in (Masrur et al., 1998a, Masrur et al., 1998b) are extended to take into account the quantitative analysis of three-phase, low torque 400Hz induction machines using data from commercially available technology. Consideration is also given to the use of HFAC for high torque motors such as those employed as part of an electrically power assisted steering (EPAS) system in which the use of low torque 400Hz machines would be inappropriate. An experimental study is undertaken into a modified column-assist EPAS system that employs a permanent magnet synchronous motor (PMSM). The aim of this study is to validate the Matlab Simulink model of the synchronous motor for the speed and torque profiles associated with different steering manoeuvers. Subsequently, the model is used to assess the voltage harmonic content and motor torque ripple of the standard DC/AC inverter, compared to a HFAC/AC drive based on zero-voltage switching.

The paper is structured as follows: section II includes a brief system description and overview of the main sub-systems within a HFAC power architecture. Section III is dedicated to the analysis of HFAC for motor

loads, and is divided into two parts: section III.1 includes a comparative analysis of DC and 400Hz AC machines, and section III.2 looks at the feasibility of a HFAC drive for the case study of an EPAS system. Section IV summarises the main findings and critically evaluates the advantages and drawbacks of HFAC power for motor-actuated auxiliary loads in passenger vehicles.

II. HFAC SYSTEM DESCRIPTION

As illustrated in Figure 1, the present 14V DC electrical system has a centralised topology. The majority of the loads are connected to the main bus in a point-to-point architecture through switches and relays, whereas the ignition and engine motor starter have direct power links.

Besides the limited power capability discussed in Section I, the 14V DC system has several major shortcomings. First, the centralised topology leads to an expensive, complex and heavy wiring harness. Second, the bus voltage level can oscillate between 9V and 16V depending on the engine speed, alternator output current, battery age and state of charge. This imposes an overrated design of the load components since the auxiliaries, aimed to operate at the nominal 14V voltage, have to cope with significant changes in the bus current (Miller et al., 1999). For example, tier one suppliers indicate an operating voltage interval of 6V to 14V for a typical fuel pump and 8V to 16V for automatic transmission actuators. Other disadvantages include the high failure rate of connectors, and the expensive and time consuming process of assembly, fault tracing and repair as further noted by Miller et al. (1999).

These problems can be solved by the replacement of the current 14V DC system with a HFAC network. The concept architecture for the proposed power bus is illustrated in Figure 2. As opposed to the DC power net, the HFAC architecture employs a distributed topology where DC power is converted to AC and then transmitted on the main bus at high frequency. The required converters, transformers, rectifiers and filters are then allocated at each point of use.

For the present analysis, a HFAC system based on a single-phase sinusoidal voltage distribution at 100V and 50kHz is considered. From an electromagnetic interference (EMI) perspective, due to its lower harmonic content, it can be argued that a sinusoidal voltage waveform is preferable to a square-wave voltage waveform (Kokes, 1997). In addition, a high distribution voltage is preferable in order to reduce the resistive losses within the distribution cable. The exact value of voltage amplitude was chosen in accordance with the SAE J2232 standard (SAE, 1999). In addition to being above the audible limit of 20 kHz, the rationale for choosing 50kHz as the bus frequency is based on a compromise between the two conflicting requirements of low conductor weight and high transmission efficiency. As illustrated in Figure 3 and detailed further in this section, the higher the frequency used, the lower the current skin depth and therefore lighter weight flat cables can be employed within the

vehicle. However, the reduction in conductor size is accompanied by a higher impendence, which affects the voltage drop and resistive losses in the distribution sub-system, and possibly a greater financial cost for the OEM.

The main components of a HFAC system are the DC/HFAC inverter, the HFAC distribution bus and the HFAC/DC or HFAC/AC converters serving as the interface between the power bus and the respective DC or AC loads. The functionality of these subsystems is briefly outlined below for reference.

DC/HFAC inverters typically employ either hard or soft switching techniques to transform the DC into sinusoidal or square-wave HFAC. As opposed to the hard switching method, in the soft switching approach the power MOSFETs or IGBTs change state when either the voltage or current across the switch is zero. As detailed in (Antaloae et al., 2010a), one downside of soft-switching inverters is the high voltage and current stress on the resonant circuit components that transform the DC voltage into resonant DC voltage.

Although the inverter presented by Kokes (1997) has been shown to be suitable for loads up to 4kW, this type of hard-switched inverter has the disadvantage that it is comparatively less efficient and is more susceptible to EMI than an equivalent inverter that employs a soft-switching strategy. An example of such a circuit, which can potentially be employed in an on-board HFAC architecture, is the resonant-switch DC/HFAC inverter, discussed in (Antaloae et al., 2010a) and shown in Figure 4 for reference. The converter can supply up to 4kW in the form of a 100V, 50kHz sinusoid from a 42V DC source. A detailed study into the performance of the circuit shows that an efficiency greater than 90% for a wide output range of loads is obtainable.

With respect to the distribution network, when selecting the HFAC conductor, consideration must be given to the skin effect that is present when a high frequency supply is used. It is known that at frequencies in the kilohertz range, current will only flow through a smaller conductor area than the one physically available (Sudipta et al., 2007). Consequently, it is deemed that the use of flat electrical conductors is best suited for HFAC power distribution (Antaloae et al., 2010b).

HFAC converters can interface low or high DC and AC voltage loads, as well as low or medium frequency (50Hz, 60Hz and 400Hz) AC motor loads, induction heating systems or current-fed applications such as LED lamps. These converters are typically based on the pulse density modulation (PDM) technique and have been extensively investigated for aerospace, naval and telecommunication electrical systems. In fact, the use of 400Hz components within the vehicle could leverage the existing component supply base infrastructure from these application areas.

HFAC/DC synchronous rectifier devices based on zero-current switching (ZCS) can supply the DC voltage or current fed ancillaries (Sood and

Lipo, 1988, Jain et al., 1993, Drobnik, 1994, Mei et al., 2002). Conversely, HFAC/AC converters utilising zero-voltage switching (ZVS) can synthesize a lower frequency supply from the HFAC bus (D. D. Renz, 1983, Agrawal et al., 1992). The cited studies indicate efficiency figures above 90% for these converters. For reference, Figure 5 illustrates the schematic diagrams of common PDM converters, including HFAC to DC, one-phase and three-phase low frequency AC.

However, the weakness associated with the use of HFAC is that the basic switching element within the converter must withstand voltages and currents in both directions and therefore two inverse-series MOSFETs or IGBTs must generally be used (Bose et al., 1996). Likely consequences of this requirement can be related to an increase in circuit cost, complexity, durability and conduction losses. In addition, potential reliability issues can arise due to the increased number of switching elements within the circuit.

III. MOTOR LOADS

This section discusses the feasibility and potential benefits associated with the use of HFAC for motor actuators within vehicles. Consideration is first given to low torque actuators as used in electric radiator fans and pumps, before extending the discussion to take into account the integration of HFAC within high-torque applications as in an EPAS system.

III.1. Low torque motor loads

Automotive applications such as electrically driven cooling fans, pumps and windscreen wipers generally employ 14V DC motors with a rated torque characteristic that peaks under 2Nm. The authors propose that such actuators can be replaced by more compact 400Hz, AC induction machines interfaced from the HFAC bus by either a three-phase or a single-phase frequency converter.

III.1.1 *Feasibility analysis of 400Hz motors*

AC machines can be interfaced from the HFAC bus by ZVS frequency converter circuits, also known as cycloconverters. The functionality of such devices is well document in the literature (D. Renz, 1983, Agrawal et al., 1992, Bose et al., 1996) and will therefore not be repeated here. For reference, Figure 6 presents example circuit topologies for both a three-phase and a single-phase cycloconverter. Figure 6 shows how a two-leg inverter can be used to couple a single-phase AC machine to the HFAC bus. Conversely, if three-phase AC machines are to be employed, then a three-leg converter is required. Irrespective of the number of current paths within the cycloconverter, as discussed in Section II, two inverse series MOSFETs form the integrated switching element. By means of an example, Figure 7 shows the resulting typical three-phase 115V voltage for a 400Hz induction motor, which has been stepped up and synthesized from the 100V, 50kHz sinusoid.

If 400Hz AC motors are to feasibly replace the present low torque DC motors in vehicles, they must offer the same torque-speed characteristics that are found within today’s DC machines. It is

known that the starting torque output of a DC machine can be considerably higher than that found within a comparable AC induction motor (Masrur et al., 1998a), and therefore it is necessary to determine under what conditions AC machines may successfully take the place of DC motors. For this purpose, performance data has been collected from a wide range of commercially available AC and DC machines, appropriate for use within automotive applications. Tables 1 and 2 include the operating point, size and potential use in the vehicle for the DC and AC induction machines, respectively. For the particular case of a 40Ncm DC motor, as employed for example in a throttle valve control actuator (Iles-Klumpner et al., 2006), Figure 8 presents the process associated with matching the operating envelope of the DC and AC motors. The graph includes the torque-speed characteristic for a 160W DC motor, with the nominal operating point at 40Ncm, 3700rpm (denoted as point 2 on the graph). The similar characteristic curve for the 425W induction motor, which has a nominal torque of 34Ncm at 11,100rpm is denoted as point 1. It is noteworthy that the starting torque of the two machines differs by a ratio of approximately 3:1. As shown in Figure 8, if a suitable gear reduction ratio is integrated within the AC motor, its nominal operating position shifts from point (1) to point (1') and the starting torque increases to more than 200Ncm. Figure 8 highlights also that with the inclusion of a fixed gear reduction, the torque capability of the AC motor increases threefold compared to the DC counterpart in the 1,000rpm to 3,000rpm region. In particular, the torque capability of the two candidate machines for a rotational speed of 2,000rpm is 255Ncm and 85Ncm, respectively. Values in this region can be a potential benefit for the throttle valve actuator. Table 3 presents a summary of the relevant data-set for this exercise and shows that with the appropriate gear ratio a 425W AC machine can successfully meet the specified stall and nominal torque requirements for the automotive application.

Repeating the steps above for a wider selection of motors, the study shows that 400Hz induction motors meet the torque specification of DC machines of up to approximately 180W. Beyond this limit, AC motors fail to meet the high starting torque requirement of the DC motors. This conclusion is supported by other studies contained within the literature (Masrur et al., 1998b). Although the majority of motor loads require less than 200W, including fuel pumps, electric cooling fans, window and seat motors, blower and windscreen wiper motors (Bosch, 2004), there are also DC machines with a higher power rating than the above threshold. For example, the power rating of motors found in electric water pumps and oil pumps can extend to as much as 500W (Lukic and Emadi, 2002, Lukic and Emadi, 2003, Miller and Nicastri, 1998). Therefore, based on present motor technology, off-the-shelf 400Hz machines are feasible to replace DC motors with a maximum stall and nominal torque capability of 4Nm and 2Nm, respectively. However, it should be noted that future technological improvements can possibly extend these limits, since the suggested nominal torque limit for a similar analysis

conducted more than a decade ago was only 0.9Nm (Masrur et al., 1998b).

III.1.2 *Benefits of 400Hz induction motors*

For equivalent 400Hz AC machines, Figure 9 presents the potential reduction in packaging volume within the vehicle as a function of the machine's power rating. The Figure shows that a significant reduction, in the order of 60%, is realisable. A similar reduction in the weight of the electrical machine can also be achieved via the transition from a DC machine to an AC induction motor (Masrur et al., 1998a). As shown in Table 1, within an automotive context, the mass of individual DC machines was found to be typically between 0.4kg – 1.5kg. Therefore, considering an average mass of 1kg per DC motor, and that up to 50 such devices may be integrated within a typical passenger vehicle, the potential vehicle weight saving can be estimated to be approximately 30kg, which is a noteworthy advantage. It should be highlighted that this is only a first-order approximation and it is based on the assumption that the AC machines detailed in Table 2 include the required gear reduction mechanism.

In addition to the possible reductions in system weight and packaging volume, Figure 10 highlights efficiency improvements between 25% and 100% associated with the use of 400Hz induction motors as compared to DC machines. Efficiency data for commercially available motors are available only for their respective nominal operating points. It can be assumed that the machines will operate in a close vicinity of their nominal, i.e. most efficient, operating region. Assuming an average power rating of 100W for continuously operating low-torque DC motors, and considering the possible mean energy saving of 30% based on Figure 10, the potential power saving for such machines is in the order of 30W per device.

However, in order to determine a more accurate estimate of the system efficiency, consideration should be given to the duty cycle of the different motor actuators. Specifically, whereas loads such as the fuel pump have a continuous duty cycle, applications including windscreen wipers or power windows are only operated on an intermittent basis. Using the information contained in (Bosch, 2004) on power consumption for different electrical consumers in vehicles, a duty cycle of 0.3 has been identified as an appropriate value for motors running intermittently. Consequently, a potential individual saving of approximately 10W for such machines can be achieved. As a result, considering the estimated saving of 30W and 10W for each continuous and intermittent machine and noting that only a small proportion of motor loads have a continuous operation, the total potential power saving for a typical vehicle may be in the region of 500W.

The efficiency improvements shown do not take into account the small losses caused by the gear reduction integrated with the AC motors, nor the conduction losses within the cycloconverter. However, the efficiency of a fixed ratio transmission is typically high, in the order of 97% (Jordan, 1994). Also, for the maximum

output power of 181W considered in this exercise, the cycloconverter current is 1.6A at 115V; since only the upper or lower side in each converter leg is conducting at any given moment, only 6 power MOSFETs are simultaneously in the on-state. As a result, for 1.6A and for a MOSFET with an internal resistance of 40mΩ, the total I^2R losses for the circuit peak at just 0.62W.

The HFAC/three-phase AC cycloconverter (illustrated in Figure 6) can be either integrated with each AC motor in modules operating as separate entities, or a single cycloconverter can be used and all motors connected to the 3-phase 400Hz AC bus. Although the latter method is initially less expensive, due to the employment of a single frequency converter, the former approach is potentially more attractive since the modules can be used in a plug-and-play mode. This can lead to an effective maintenance procedure, which in turn may save cost over the lifetime of the vehicle.

Conclusively, based on a number of assumptions regarding to the number of electrical motors in the vehicle and the duty cycle of the majority of these, potential vehicle weight and electrical power saving in the region of 30kg and 500W can be realised, respectively. Also, since the 400Hz machines are proposed as replacement for brushed DC motors, EMI can be improved as well as the overall reliability of the system.

Based on the fact that approximately 5% of the fuel consumed in a medium-sized automobile is used to drive the alternator and transport the combined weight of the starter, battery and alternator, approximately 0.1L/100km can be attributed to every 10kg added to the vehicle or 100W of drive power (Bosch, 2004). Mapping the figures above to these potential savings in terms of weight and electrical power associated with the use of 400Hz motors, a possible fuel consumption saving of approximately 0.8L/100km (or extended vehicle range by 5 miles per imperial gallon) is feasible.

Several aspects should be noted with regard to the three-phase AC system supplying the 400Hz AC motors. First, additional weight and packaging volume can potentially be saved at the power distribution level, since the three-phase AC system requires less copper than a DC system to distribute the same amount of power (Miller, 1996). Also, the three-phase system is more fault-tolerant: if one of the lines breaks down, power distribution is degraded but nonetheless can be maintained by the remaining two lines. However, a possible issue related to the three-phase system is that it may require a load-balancing mechanism amongst the phases.

III.2 High torque motor drives

Within the context of the present analysis, high torque refers to applications with a rated requirement above the 2Nm capability of 400Hz AC induction machines. Such loads include, for example, existing consumers such as EPAS (7Nm), air-conditioning (6Nm) and proposed state-of-the-art systems such as brake-by-wire, variable valve timing (VVT), electromechanical active suspension or the full electric gearbox. All of these applications integrate motors with a

rated torque of 3Nm, 4Nm, 50Nm and 120Nm, respectively (Iles-Klumpner et al., 2006, Murakami et al., 2001).

As a result, within such applications high torque actuators are used. These may include permanent magnet (PM) DC or three-phase interior or surface-mounted permanent magnet machines. For example, a 320W PM DC motor has been shown to be feasible as a possible VVT actuator (for one valve) (Chang, 2003); also, it has been reported that a three-phase, surface-mounted PM AC machine rated at 3.1kW is suitable for the heating, ventilation and air conditioning (HVAC) system in vehicles (Naidu et al., 2003). It is noteworthy that these high torque applications require a higher voltage than the current 14V. Particularly, for the two examples above, a 42V DC supply has been considered a pre-requisite.

In order to interface such actuators from the HFAC bus, two methods can be employed. A first possibility is to transform the HFAC into DC, using ZCS synchronous rectifiers as described in Section II, which in turn supplies a high-torque PM DC motor. The alternative approach is to utilise an existing three-phase AC machine, but replace the standard DC/AC inverter with a HFAC/AC drive. Such an inverter can synthesise the low-frequency AC from the HFAC based on ZVS and PDM. The second solution is preferable to the former as the intermediary stage of converting HFAC to DC can be eliminated. In addition, since soft switching is used, a HFAC/AC converter is expected to offer benefits such as lower voltage EMI and reduced motor torque ripple in comparison to the equivalent DC/AC bridge.

In order to test these assumptions, a typical high torque load has been considered: the EPAS application, which is a standard technology on the majority of vehicles today either as a full-electric or electro-hydraulic system. Both PM DC and PM AC motors are suitable for EPAS, although the latter in the form of a surface-mounted PM synchronous motor (PMSM) is the preferred choice due to its high specific torque, coupled with high efficiency and low torque ripple (Liu et al., 2004, Hur, 2008). The torque oscillation is a performance attribute of particular interest, since it causes not only an audible noise, but also mechanical vibration within the steering column which is propagated through to the steering wheel (Bianchi and Bolognani, 2000).

To support this study, an experimental test-rig of a production EPAS system is employed to create a realistic load profile for the PMSM actuator. This setup is described further in Section III.2.1. Subsequently, in Sections III.2.2 to III.2.6, a mathematical model of the experimental apparatus is described and used to extend the study by providing an insight into the operation of HFAC/AC and DC/AC drives for the EPAS application. In particular, the model is used to compare the voltage harmonic content and the PMSM torque ripple associated with the two drives.

III.2.1 *EPAS Experimental Apparatus*

The experimental column-assist EPAS system is shown in Figure A.1 and it includes a variable

load in the form of a hydraulic circuit that emulates the typical road forces associated with different steering manoeuvers. The original production motor attached to the steering column was a 14V, 300W PM DC motor. As part of the study, this machine was replaced with a bespoke three-phase 440W PMSM machine. Information relating to the design of this machine, which is shown in Figure A.2, is discussed in (Wang et al., 2010) and will therefore not be repeated here. The full list of machine parameters is included in Table A.1. The relevant machine parameters appropriate for this study are summarized below for reference:

- open-circuit phase voltage 12.5V;
- phase current 13A;
- base speed 62.8rad/s (600rpm);
- nominal torque 7Nm;

A schematic diagram showing the main components, connections and control of the EPAS system is depicted in Figure 11. The hydraulic subsystem emulates the variable load of the EPAS systems by means of two needle valves. These valves control the bi-directional flow and hence the pressure within the circuit. An off-the-shelf device controls the PMSM torque based on two inputs; first, a reference motor current is set using the associated computer software, and second the rotor position signal from the encoder attached to the PMSM.

Using the experimental apparatus, discussed above, a comprehensive test programme was undertaken using a 48V DC power supply. The reason for a higher voltage level than 42V DC is that 48V is the minimum required by the controller. The results of this activity were used to validate the equivalent EPAS DC model built within Matlab Simulink. The following section describes the construction and implementation of the mathematical model.

III.2.2 *Description of the EPAS Model with DC/AC Drive*

The Matlab Simlulink EPAS model includes three main sub-systems, which build upon the existing SimPowerSystems toolbox. A high-level diagram of the model is shown in Figure 12.a and includes:

- the representation of the PMSM motor, described in Section III.2.1;
- the power electronics subsystem, which implements both the motor control scheme and the DC/AC bridge, and finally
- the subsystem that emulates the load torque for the PMSM,

The latter component of the model is represented as a torque vs. speed lookup table that has been derived from experimental results.

The torque control is achieved via the vector control technique, which is considered superior to other regulation methods such as Volts/Hertz, sensorless vector or flux vector control, and has been extensively described in the literature (Emadi, 2005). For reference, a schematic diagram of this control method is illustrated in Figure 12.b. Block A, which relates to the vector control, is based on the Clarke and Park

transformations method of converting the three-phase motor currents into the *d* and *q* axes components. The current component along the *q-axis* is directly proportional to the motor torque and the current component along the *d-axis* is directly proportional to the motor flux. Therefore, *iq ref* shown in Figure 12.b represents the torque command to the control system. In addition, since the rotor flux is fixed (determined by the physical properties of the magnets employed within the PMSM), the current reference along the *d-axis* is set to zero (Emadi, 2005).

An important block in the control scheme in Figure 12.b is the modulation model. Typical strategies include sinusoidal and space vector (SV) methods, based on pulse width modulation (PWM). It has been reported in the literature that the latter (SV PWM) offers superior performance in terms of low voltage total harmonic distortion (THD), torque ripple, switching losses and high output-to-input voltage ratio (Emadi, 2005, Tsung-Po et al., 1999). Therefore, this modulation technique has been implemented in the control model.

III.2.3 *Validation of the EPAS Model with DC/AC Drive*

Several tests have been carried out in order to validate the Simulink mathematical model. Experimental and simulation waveforms associated with four tests are illustrated in Figure 13, and include steady state motor current of 1A and 2A, and current step tests from 3A to 4A, and 4A to 6A.

Each test has been performed at a different pressure level in the hydraulic circuit, and is representative for the varying load conditions within the EPAS system (e.g. high or low motor load for parking maoeuvers or urban driving, respectively). In particular, by adjusting the flow in the hydraulic circuit using needle valves (as indicated in Figure 11), the different road load characteristics shown in Figure 14 have been obtained for the four test scenarios and were implemented as the torque vs. speed load characteristics in the model (Block C in Figure 12).

The first two test cases (1A and 2A motor current) and the latter two experiments (3A-4A and 4A-6A) are representative for low-level and medium-level motor assist within EPAS systems for small to medium size vehicles (Eki et al., 2007). Specifically, since a constant of 2.6 has been identified as the ratio between motor current (A) and torque (Nm), the active current waveforms in Figure 13 (right) correspond to a torque range between 0.38Nm and 2.31Nm. Consequently, based on the gear ratio of 12 to 1 between the motor shaft and the steering column, and that the pinion radius in the rack-and-pinion connection equals 7mm, the forces exerted in the test hydraulic circuit for the four trials are: 650N (for 1A motor current), 1.3kN (2A), 1.95kN (3A), 2.6kN (4A) and 3.9kN (6A). It should be noted that although the motor rated torque is equal to 7Nm, the present analysis is limited to 2.31Nm due to the high stress on the mechanical components in the EPAS apparatus (Figure A.1).

As it can be seen in Figure 13, for EPAS motor torque levels appropriate for use within both small and medium-sized vehicles, a high degree of correlation exists between the experimental and simulation results. This in turn implies that the mathematical model of the DC system is representative of the physical realisation of the technology.

III.2.4 *Modification of the EPAS Model to include a HFAC/AC Drive*

The validated EPAS model described in Section III.2.2 has been extended in order to integrate a HFAC/AC drive that replaces its DC/AC counterpart. The aim of this study is to derive a comparison between the operation of the two inverter technologies, in terms of both the output voltage harmonics and the motor torque ripple. Both of these parameters, as discussed in (Bianchi et al., 2005, Graovac et al., 2008), are key to satisfactory system performance within a vehicle application.

The modifications made to the model are related only to block A of Figure 12 (a and b) and are illustrated in Figure 15a. The enhancements consist of replacing the 6-switch DC/AC inverter with a 12-switch HFAC/AC circuit (detailed in Figure 15.b). The rationale for this design decision has already been discussed in Section II. The enhancement of the SV PWM algorithm for zero-voltage switching is described below.

A common way to represent the three phase machine voltages is by using a space vector model. This technique has been extensively covered in the literature (Emadi, 2005). The main principle of this model is that the eight vectors, corresponding to the eight different states in a 3-leg DC/AC bridge, are used in pairs of two adjacent vectors to produce the desired output voltage. Every time period, the controller computes the three time variables required to bias the output voltage amplitude and direction according to the reference voltage or current. Consequently, the bridge changes state (i.e. MOSFETs are switched *on* and *off*) at these predefined time moments.

The authors propose that the SV PWM model be replaced by a SV model based on pulse density modulation of half-wave AC sinusoids, to allow for zero voltage switching in the HFAC/AC drive for reasons detailed in Section III.2. Specifically, the proposed method is based on the original SV principle; the only difference is that the three variables (denoted as *Ta*, *Tb* and *Tc*), are determined as multiples of half the fundamental time period of the high frequency AC voltage. For the present analysis, this entails that *Ta*, *Tb* and *Tc*, are calculated every time period to be multiples of 10μs.

Figure 16a illustrates the typical state change of the three legs in a DC/AC inverter for one time period, where the *zero* state is equivalent to the low-side MOSFET conducting and state *one* indicates when the high-side MOSFET is switched *on.* As it can be seen from Figure 16b, for the same scenario, the proposed SV PDM algorithm ensures that switching is aligned with the 50kHz bus frequency,

III.2.5 *Comparison between the DC/AC and HFAC/AC Drives for the EPAS system*

Figure 17 shows the comparison between voltage, current, torque, speed and the voltage harmonic content associated with the DC drive (left hand side) and the HFAC drive (right hand side of the Figure) for the case study of a step motor current from 4A to 6A. The implementation of the model is shown, for reference, in Figures A.3a and A.3b.

As it can be seen from Figures 17e and 17f, although the SV PDM algorithm is feasible for the EPAS HFAC/AC drive and allows for ZVS, the motor torque ripple appears to be higher compared to the DC/AC inverter. The Figure shows that for a steady-state torque output, the peak-peak motor torque is in the order 0.07Nm when controlled via HFAC drive. This is 1.7% and 1.2% greater than that observed before and after the time step, respectively, when the machine is supplied from the DC/AC inverter, which implies that the higher mechanical vibration will be present within the steering column and therefore in the steering wheel. However, the overall torque ripple for the HFAC drive is 5% and 3.1% for a PMSM torque of 1.53Nm and 2.31Nm, respectively, which is within the 5% requirement for an EPAS implementation (Hur, 2008).

The higher motor torque ripples associated with the HFAC drive can be accounted for by the modification of the SVM technique for loss-less switching of the AC voltage. As described in Section III.2.4, the three time constants *Ta*, *Tb* and *Tc* are computed at the beginning of each time period and are constrained to be multiples of 10μs. The consequence is that the HFAC voltage applied to the PMSM has a lower resolution in comparison to the DC voltage; small differences between the two drive voltages can also be observed in Figures 17a and 17b.

It should be noted that it is possible to achieve the same level of output torque ripple by applying the non-modified SVM algorithm to the HFAC/AC converter. While this has the advantage of reducing the torque oscillations, the disadvantage is that it requires the use of non-ZVS within the HFAC/AC drive, which in turn degrades the efficiency of the electrical sub-system by adding switching losses to the overall bridge losses.

The frequency spectrum of the hard-switched and synthesized AC voltage (sampled at a frequency of 500kHz) across the motor windings is illustrated in Figures 17i and 17j, respectively. The plot includes frequencies up to 250kHz, and it shows that although the frequency spectrum of the DC voltage is lower than the equivalent of the HFAC/AC system above 50kHz, it includes comparatively lower frequency components below this threshold (by approximately 10%). It has been indicated in the literature that the high frequency harmonics can be easily filtered out (Sudipta et al., 2007). Furthermore, it has been suggested that reduced harmonics in the lower frequency range can potentially reduce the motor copper losses (Venkatesan and Lindsay, 1982), especially for high machine torque levels.

The HFAC/AC drive based on soft switching techniques offers simultaneous advantages such as low voltage harmonic content below a frequency of 50kHz and no switching losses. In particular, based on equation (1), Figure 18 illustrates the associated switching losses for a DC to three-phase AC drive circuit for several switching frequencies and load currents up to 60A. It can be observed that the maximum switching loss, which occurs at 60A and 20kHz switching frequency, is approximately 13W.

Switching power losses = Switching frequency x (P_on x T_on + P_off x T_off)
(1)

P_on and *P_off* in equation (1) are the turn-on and turn-off MOSFET switching losses (W). These values were obtained from the measurement of a typical voltage and current waveform in a power MOSFET, as shown in Figure A.4 (Lourdes, 2010). It was found that *P_on* and *P_off* are approximately equal to $0.5 \cdot V \cdot I$, where V is the voltage across the MOSFET before it changes state, and I is the current in the MOSFET. The turn on and turn off times, *T_on* and *T_off* , have been measured as 118ns and 51ns, respectively.

Regardless of the elimination of switching losses, since the HFAC/AC drive employs twice as many power MOSFETs as the DC/AC equivalent circuit, it follows that its conduction losses are effectively double. A typical MOSFET for the EPAS application with an internal resistance of 42mΩ will dissipate 4.2W at 10A, and 16.8W for a load current of 20A, which is higher than the maximum possible saving of 13W at 60A in switching losses. This limitation becomes more apparent when all the 12 switches are considered. Specifically, for a load current of 6A, the I^2R losses are 4.5W and 9W for the DC/AC and the HFAC/AC converters, respectively. The same figures are 50W and 100W, respectively, for a load current of 20A, which is a significant disadvantage for the use of a HFAC drive.

In summary, this section has highlighted that HFAC can bring both advantages and disadvantages for high-torque motor electrical loads. The main advantage is a reduced low-frequency harmonic content in the supply voltage to the actuator, and although switching losses can be avoided, the conduction losses, which are predominant, are effectively double in comparison to the DC/AC drive since it makes use of 12 power MOSFETs instead of 6. Although this disadvantage is inherent in the physical design of the system and can therefore not be mitigated against by the use of novel switching strategies, potential motor energy savings are still feasible due to the reduced voltage harmonics in the lower frequency range (under 50kHz).

Furthermore, the shortcomings associated with the use of a HFAC/AC system stem from the need to satisfy the conflicting requirements of high performance and high efficiency. If a ZVS strategy is employed to increase system efficiency, the side-effect of this is a higher torque ripple in the output of the electrical machine. In order to reduce the magnitude of

the torque oscillations (to a value comparable to that associated a DC/AC drive) a hard switching strategy must be employed. It is noteworthy however, that the increase in output torque ripple is still below the 5% maximum threshold, cited by (Hur, 2008) for an EPAS application.

Based on the results of the study presented in this subsection, it is concluded that, as yet, there are no tangible performance or efficiency benefits associated with the use of HFAC instead of DC for high-torque motor applications. In addition, the level of control complexity required to manage the HFAC drive may further negate its future adoption by the automotive sector. Therefore, either HFAC/DC synchronous rectifiers or HFAC/DC/AC converters are recommended for use with high-torque DC or AC machines, respectively.

IV. Conclusions

The feasibility of HFAC power for two main categories of motor-actuated electrical applications has been analysed in this paper: low torque (2Nm nominal, 4Nm peak) loads and high torque (above 2Nm) loads. The rationale for this division is the limited torque capability of present 400Hz AC machine technology, which the authors propose as a replacement for DC motors with a rated torque below 2Nm.

It was shown that a significant benefit in efficiency (up to 100%), packaging volume and weight (above 60%) is feasible by replacing DC motors with commercially available AC induction motors with a nominal torque of up to 2Nm. This limit is dictated by the low starting torque capability of the AC machines, since their operating torque vs. speed profile must match the profile of the DC motors therefore to be replaced. Based on the assumptions described in Section III.1, relating to the number of electrical motors employed and their respective duty-cycles, the potential weight and electrical power saving for a typical medium size vehicle is in the region of 30kg and 500W respectively.

Section III.2 illustrated that a HFAC/AC frequency converter based on zero-voltage switching may degrade the performance of high-torque motor actuators and lead to considerable losses in the conversion process due to the high number of power MOSFETs required. Nonetheless, forgoing zero-voltage switching in the bridge, standard modulation techniques can be applied with no penalty in motor performance at the cost of added switching losses. Also, it is possible that the lower voltage harmonics (below 50kHz) of the HFAC/AC circuit compared to the DC/AC bridge may reduce the copper losses in the three-phase motor and partially compensate for the higher conduction losses. Furthermore, it has been argued in the literature that the higher harmonic content of the 12-switch HFAC/AC inverter above 50kHz can be easily removed via appropriate filtering.

In conclusion, significant benefits of HFAC can be claimed for applications integrating low-torque DC motors. Since these loads are predominant in the vehicle in comparison to high-torque actuators, an overall verdict for the present analysis is favourable for the adoption

of a HFAC bus architecture. Advantages in terms of weight and efficiency are obtainable, which in turn support the overall strategy of many OEMs towards the market introduction of more fuel-efficient vehicles.

Acknowledgements

The research presented within this paper is part of the HIFPADD project, funded by the Technology Strategy Board in the UK.

REFERENCES

R

AGRAWAL, V., AGARWAL, A. K. & KANT, K. (1992) A study of single-phase to three-phase cycloconverters using PSPICE. *Industrial Electronics, IEEE Transactions on,* 39**,** 141-148.

ANTALOAE, C., MARCO, J. & VAUGHAN, N. D. (2010a) High Frequency Alternating Current Power Supply for Automobile Auxiliary Electrical Systems. *International Symposium on POWER ELECTRONICS, ELECTRICAL DRIVES, AUTOMATION and MOTION.* Pisa, Italy, IEEE.

ANTALOAE, C., MARCO, J. & VAUGHAN, N. D. (2010b) Investigation of High Frequency AC Power Distribution Benefits for the Automobile Auxiliary Electrical System. *SAE Int. J. Passeng. Cars – Electron. Electr. Syst.,* 3**,** 109-121.

BIANCHI, N. & BOLOGNANI, S. (2000) Design techniques for reducing the cogging torque in surface-mounted PM motors. *Industry Applications Conference, 2000. Conference Record of the 2000 IEEE.*

BIANCHI, N., BOLOGNANI, S. & DAI PRE, M. (2005) Design of a Fault-tolerant IPM Motor for Electric Power Steering. *Power Electronics Specialists Conference, 2005. PESC '05. IEEE 36th.*

BOSCH (2004) *Bosch automotive handbook*.

BOSE, B. K., MIN-HUEI, K. & KANKAM, M. D. (1996) High frequency AC vs. DC distribution system for next generation hybrid electric vehicle. *Industrial Electronics, Control, and Instrumentation, 1996., Proceedings of the 1996 IEEE IECON 22nd International Conference on.*

CALISKAN, V. (2000) A Dual/High-Voltage Automotive Electrical Power System with Superior Transient Performance. *Department of Electrical Engineering and Computer Science.* Massachusetts Institute of Technology

CHANG, W. S. (2003) An Electromechanical Valve Drive Incorporating a Nonlinear Mechanical Transformer. *Department of Electrical Engineering and Computer Science.* Massachusetts Institute of Technology

D. D. RENZ, R. C. F., N. OOHN STEVENS, JAMES E. TRINER, AND IRVING6. HANSEN (1983) DESIGN CONSIDERATIONS FOR LARGE SPACE ELECTRIC POWER SYSTEM. NASA Lewis Research Center Clevelnd.

D. RENZ, R. C. F., N. OOHN STEVENS, JAMES E. TRINER, AND IRVING6. HANSEN (1983) DESIGN CONSIDERATIONS FOR LARGE SPACE ELECTRIC POWER SYSTEM. NASA Lewis Research Center Clevelnd.

DOUBLET, L., JEMAA, N. B., HAUNER, F. & JEANNOT, D. (2004) "Electrical arc phenomena and its interaction on contact material at 42 volts DC for automotive applications". *Electrical Contacts, 2004. Proceedings of the 50th IEEE Holm Conference on Electrical Contacts and the 22nd International Conference on Electrical Contacts.*

DROBNIK, J. (1994) High frequency alternating current power distribution. *Telecommunications Energy Conference, 1994. INTELEC '94., 16th International.*

EKI, H., TERATANI, T. & IWASAKI, T. (2007) Power Consumption and Conversion of EPS Systems. *Power Conversion Conference - Nagoya, 2007. PCC '07.*

EMADI, A. (2005) *Handbook of Automotive Power Electronics and Motor Drives*, CRC Press, Taylor & Francis Group.

EMADI, A., EHSANI, M. & M.MILLER, J. (2004) *Vehicular Electric Power Systems: Land, Sea, Air, and Space Vehicles*.

GRAOVAC, D., KOPPL, B., SCHEFFER, M., KIEP, A. & PURSCHEL, M. (2008) Optimal PWM method for electric and electro-hydraulic power steering applications. *Power Electronics Specialists Conference, 2008. PESC 2008. IEEE.*

HONEYWILL, T. (2007) Down to the wire. *Automotive Engineer.* UK, Professional Engineering Publishing Limited (publishing company of the Institution of Mechanical Engineers).

HUR, J. (2008) Characteristic Analysis of Interior Permanent-Magnet Synchronous Motor in Electrohydraulic Power Steering Systems. *IEEE Transactions on Industrial Electronics,* 55.

ILES-KLUMPNER, D., SERBAN, I. & RISTICEVIC, M. (2006) Automotive Electrical Actuation Technologies. *Vehicle Power and Propulsion Conference, 2006. VPPC '06. IEEE.*

JAIN, P., TANJU, M. C. & BOTTRILL, J. (1993) AC/DC converter topologies for the Space Station. *Aerospace and Electronic Systems, IEEE Transactions on,* 29**,** 425-434.

JONASSON, M. & ROOS, F. (2008) Design and evaluation of an active electromechanical wheel suspension system. *Mechatronics,* 18**,** 218-230.

JORDAN, H. E. (1994) *Energy-Efficient Electric Motors and Their Applications*, Plenum Press, New York.

KASSAKIAN, J. G., WOLF, H. C., MILLER, J. M. & HURTON, C. J. (1996) Automotive electrical systems circa 2005. *Spectrum, IEEE,* 33**,** 22-27.

KEIM, T. A. (2004) 42 Volts - The View from Today. IN ASSOCIATION, C. T. E. (Ed.).

KOKES, M. (1997) Resonantes Wecselspannungsbordnetz für Kraftfahrzeuge und dessen Beschreibung mit Zustandszeigern. Bochum University.

LINE, C., MANZIE, C. & GOOD, M. C. (2008) Electromechanical Brake Modeling and Control: From PI to MPC. *Control Systems Technology, IEEE Transactions on,* 16**,** 446-457.

LIU, G., KURNIA, A., LARMINAT, R. D., DESMOND, P. & O'GORMAN, T. (2004) A Low Torque Ripple PMSM Drive for EPS Applications. IN IEEE (Ed.). IEEE.

LOURDES, S. (2010) Isolated Mosfet Module - Test Report. Cranfield University.

LUKIC, S. M. & EMADI, A. (2002) Performance analysis of automotive power systems: effects of power electronic intensive loads and electrically-assisted propulsion systems. *Vehicular Technology Conference, 2002. Proceedings. VTC 2002-Fall. 2002 IEEE 56th.*

LUKIC, S. M. & EMADI, A. (2003) Effects of Electrical Loads on 42V Automotive Power Systems. IN INTERNATIONAL, S. (Ed.) *Future Transportation Technology Conference & Exhibition, June 2003; Session: Vehicle Power Systems and 42 Volt Technology.* Costa Mesa, CA, USA, SAE.

MASRUR, M. A., SITAR, D. S. & SANKARAN, V. A. (1998a) Can an AC (alternating current) electrical system replace the present DC system in the automobile? An investigative feasibility study. I. System architecture. *Vehicular Technology, IEEE Transactions on,* 47**,** 1072-1080.

MASRUR, M. A., SITAR, D. S. & SANKARAN, V. A. (1998b) Can an AC (alternating current) electrical system replace the present DC system in the automobile? An investigative feasibility study. II. Comparison and tradeoffs. *Vehicular Technology, IEEE Transactions on,* 47**,** 1081-1086.

MEI, Q., JAIN, P. K. & HAIBO, Z. (2002) An AC VRM topology for high frequency AC power distribution systems. *Applied Power Electronics Conference and Exposition, 2002. APEC 2002. Seventeenth Annual IEEE.*

MILLER, J. M. (1996) Multiple voltage electrical power distribution system for automotive applications. *Energy Conversion Engineering Conference, 1996. IECEC 96. Proceedings of the 31st Intersociety.*

MILLER, J. M., EMADI, A., RAJARATHNAM, A. V. & EHSANI, M. (1999) Current status and future trends in More Electric Car power systems. *Vehicular Technology Conference, 1999 IEEE 49th.*

MILLER, J. M. & NICASTRI, P. R. (1998) The next generation automotive electrical power system architecture: issues and challenges. *Digital Avionics Systems Conference, 1998. Proceedings., 17th DASC. The AIAA/IEEE/SAE.*

MURAKAMI, H., KATAOKA, H., HONDA, Y., MORIMOTO, S. & TAKEDA, Y. (2001) Highly efficient brushless motor design for an air-conditioner of the next generation 42 V vehicle. *Industry Applications Conference, 2001. Thirty-Sixth IAS Annual Meeting. Conference Record of the 2001 IEEE.*

NAIDU, M., NEHL, T. W., GOPALAKRISHNAN, S. & WURTH, L. (2003) A semi-integrated sensorless PM brushless drive for a 42 V automotive HVAC compressor. *Industry Applications Conference, 2003. 38th IAS Annual Meeting. Conference Record of the.*
PATEL, M. R. (2005) *Spacecraft Power Systems*, CRC Press.
RAJASHEKARA, K. (2003) 42 V architecture for automobiles. *Electrical Insulation Conference and Electrical Manufacturing & Coil Winding Technology Conference, 2003. Proceedings.*
SAE (1999) Electrical Systems: SAE J2232 JUN1999—Vehicle System Voltage—Initial Recommendations. SAE.
SMITH, C. R. (1991) Review of Heavy Duty Dual Voltage Systems. IN SAE (Ed.) *International Off-Highway & Powerplant Congress & Exposition.* SAE.
SOOD, P. K. & LIPO, T. A. (1988) Power conversion distribution system using a high-frequency AC link. *Industry Applications, IEEE Transactions on,* 24**,** 288-300.
SUDIPTA, C., MANOJA, D. W. & SIMOES, M. G. (2007) Distributed Intelligent Energy Management System for a Single-Phase High-Frequency AC Microgrid. *Industrial Electronics, IEEE Transactions on,* 54**,** 97-109.
TSUNG-PO, C., YEN-SHIN, L. & CHANG-HUAN, L. (1999) A new space vector modulation technique for inverter control. *Power Electronics Specialists Conference, 1999. PESC 99. 30th Annual IEEE.*
UCHIDA, M., MURATA, R., YABUMI, T., MORITA, Y. & KANDO, H. (2007) Opening and Closing Control for Electromagnetic Engine Valve. *Industrial Electronics Society, 2007. IECON 2007. 33rd Annual Conference of the IEEE.*
VENKATESAN, K. & LINDSAY, J. F. (1982) Comparative Study of the Losses in Voltage and Current Source Inverter Fed Induction Motors. *Industry Applications, IEEE Transactions on,* IA-18**,** 240-246.
WANG, C., SHEN, J., JIN, M., LUK, P. C.-K. & FEI, W. (2010) Design Issues of an IPM BLAC Motor Used for Electric Power Steering. *Fifth International Conference and Exhibition on Ecological Vehicles and Renewable Energies.* Monte Carlo.
WONG, F. K. (2004) High Frequency Transformer for Switching Mode Power Supplies. *School of Microelectronic Engineering.* Griffith University.

FIGURES

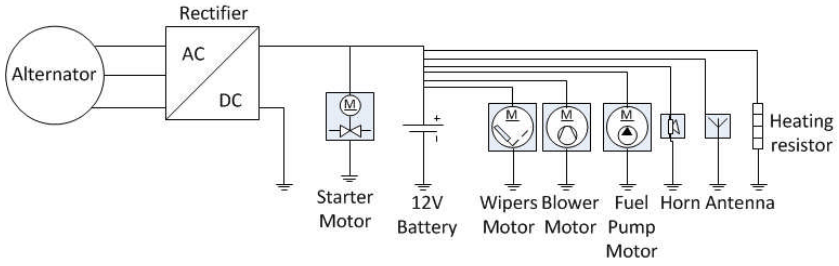

Figure 1. The present 14V DC auxiliary electrical system

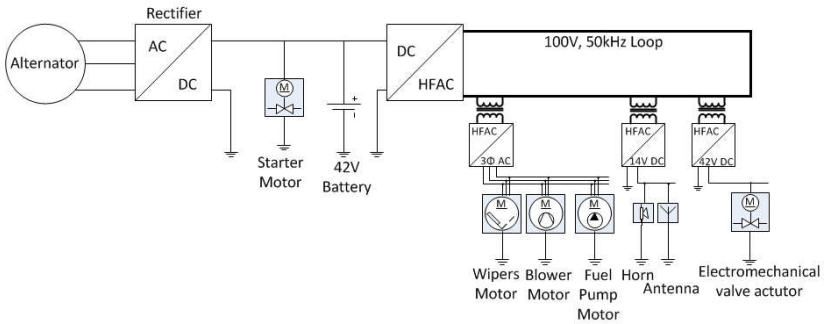

Figure 2. Proposed high frequency AC auxiliary electrical system

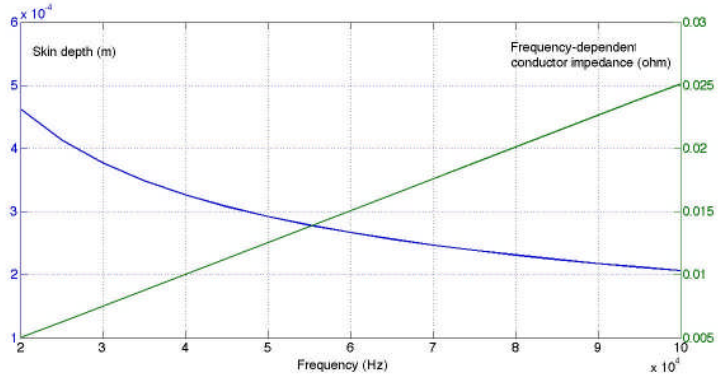

Figure 3.Skin depth (m) vs. Frequency-dependent conductor impedance (Ω), function of frequency (Hz)

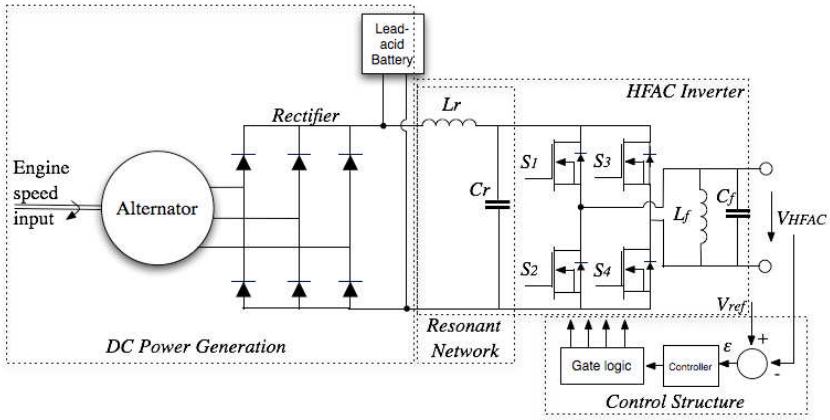

Figure 4. Possible HFAC power supply, based on resonant-switch inverter (Antaloae et al., 2010a)

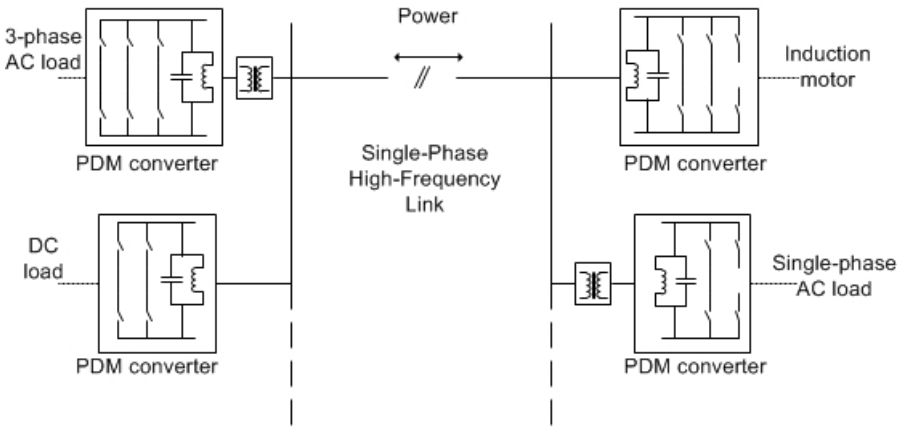

Figure 5.Pulse density modulation HFAC to DC,single and three-phase converters (Sood and Lipo, 1988)

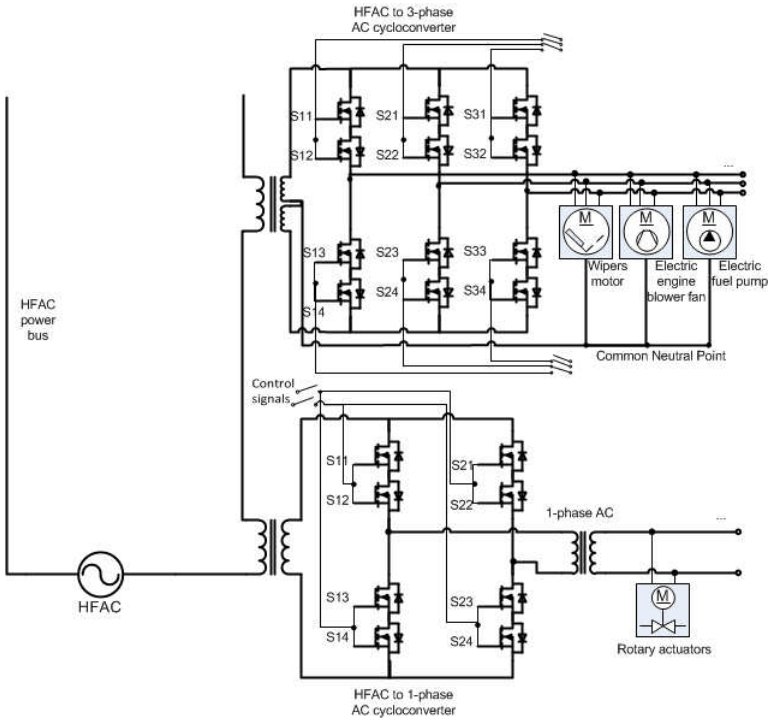

Figure 6. Schematic diagram of single and three-phase cycloconverters

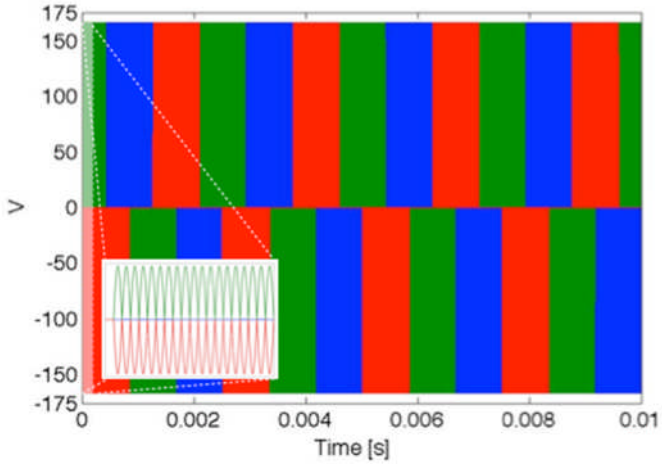

Figure 7. Synthesized 400Hz AC from 50kHz AC (Green: Phase A. Blue: Phase B. Red: Phase C)

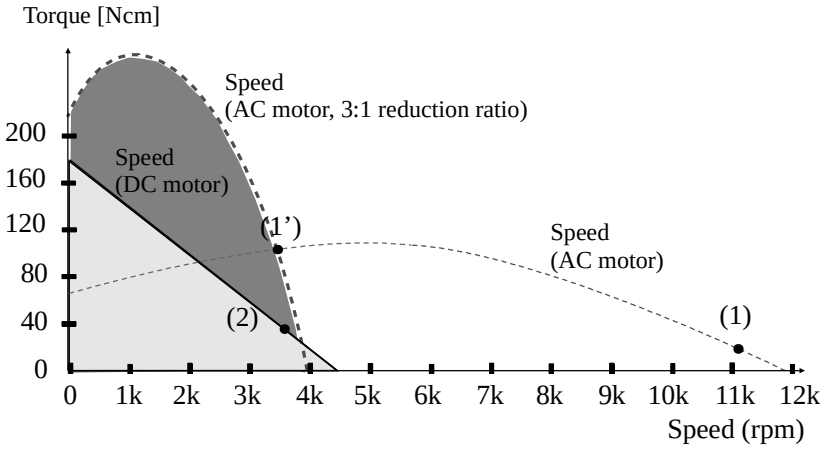

Figure 8. Operating torque vs. speed envelope of 160W DC and 425W 400Hz AC machines

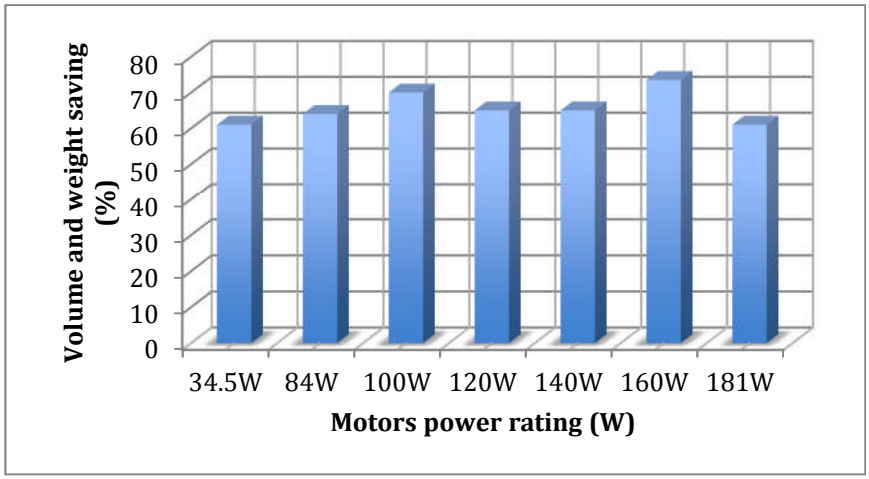

Figure 9. Potential packaging volume and weight saving of 400Hz AC machines compared to DC motors, vs. power rating (W)

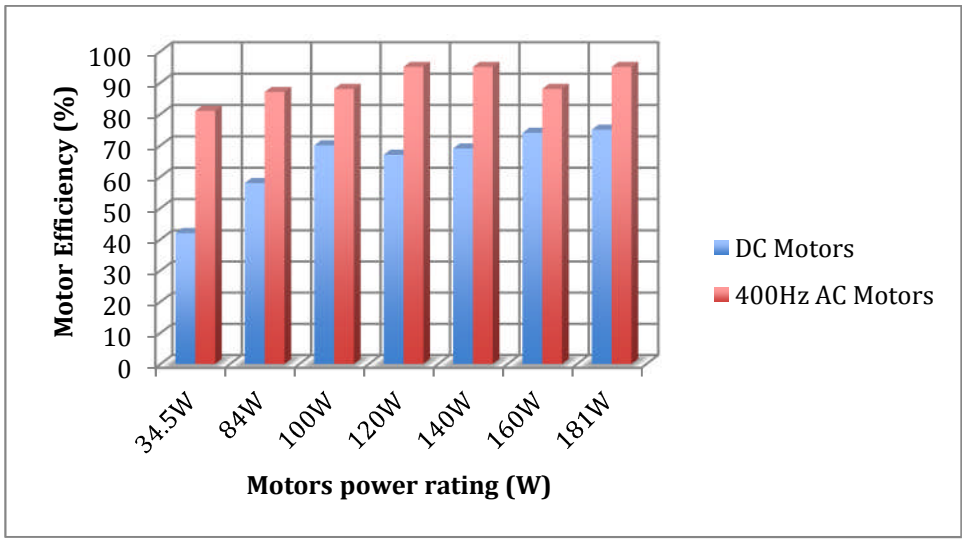

Figure 10. Efficiency of 400Hz and DC motors (at the nominal operating point) vs. power rating (W)

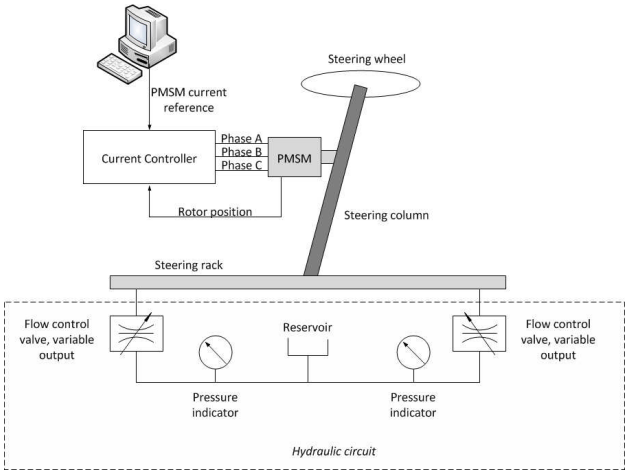

Figure 11. Diagram of EPAS experimental apparatus

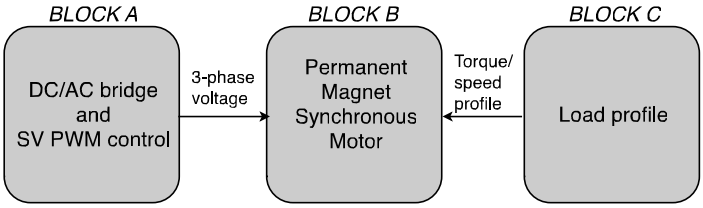

Figure 12a. Block diagram of EPAS model

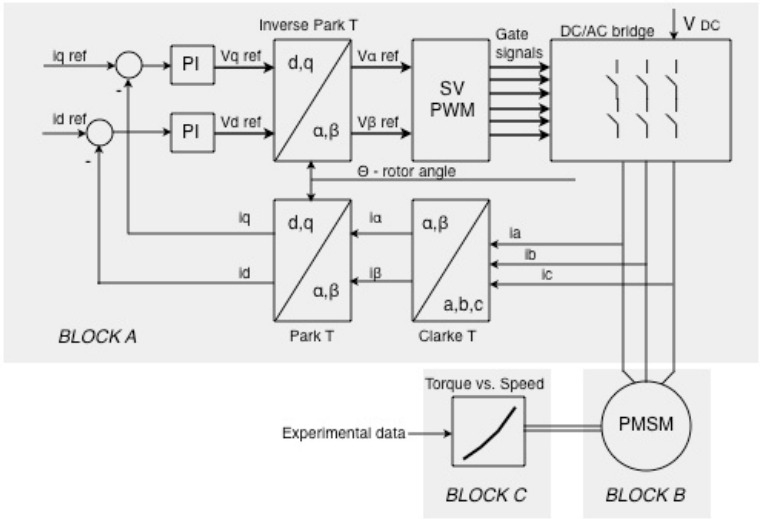

Figure 12b. Detailed block diagram of EPAS model

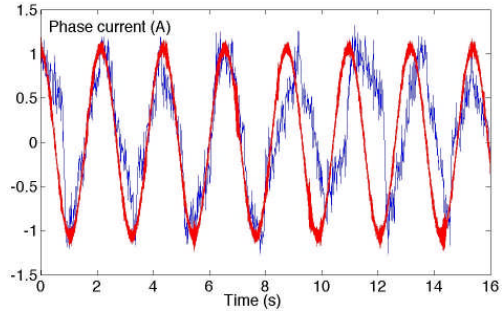

Figure 13a. 1A motor phase current (A)

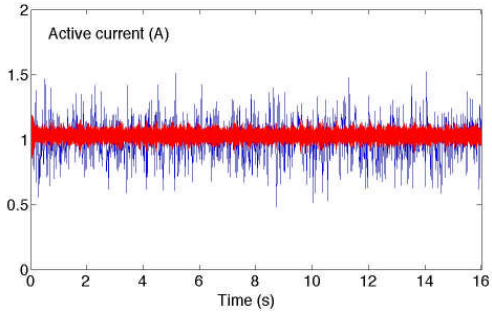

Figure 13b. 1A motor active current (A)

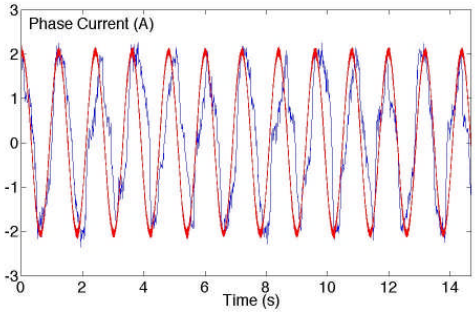

Figure 13c. 2A motor phase current (A)

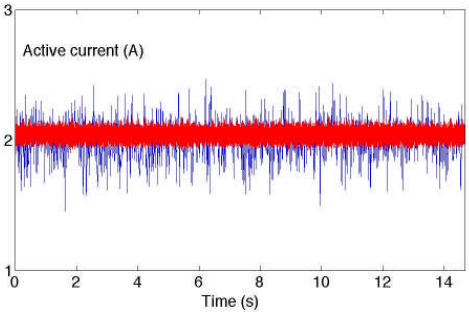

Figure 13d. 2A motor active current (A)

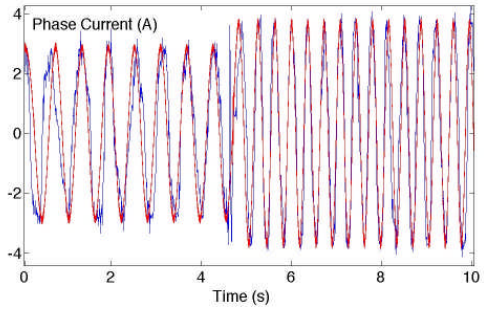

Figure 13e. 3A-4A motor phase current (A)

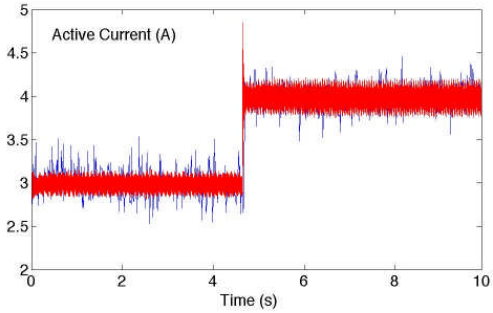

Figure 13f. 3A-4A motor active current (A)

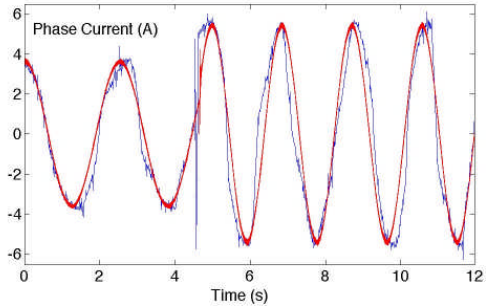

Figure 13g. 4A-6A motor phase current (A)

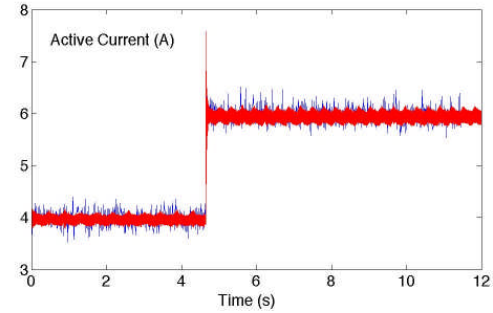

Figure 13h. 4A-6A motor active current (A)

Figure 13. Phase (left) and active (right) motor current, experimental (blue) and simulation (red) results for four tests: 1A, 2A, 3A-4A and 4A to 6A.

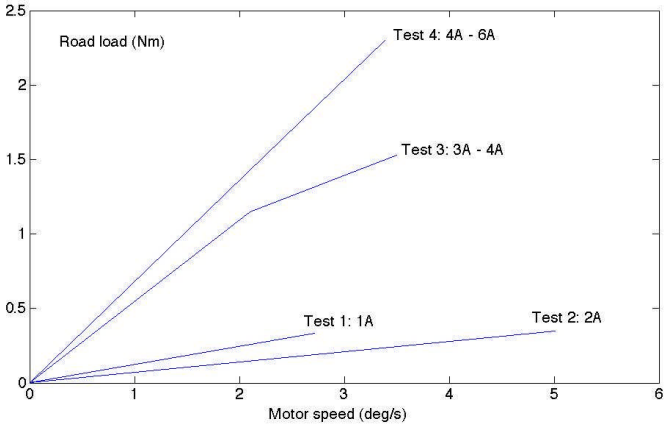

Figure 14. Load profile (*road* torque vs. motor speed) for four case studies

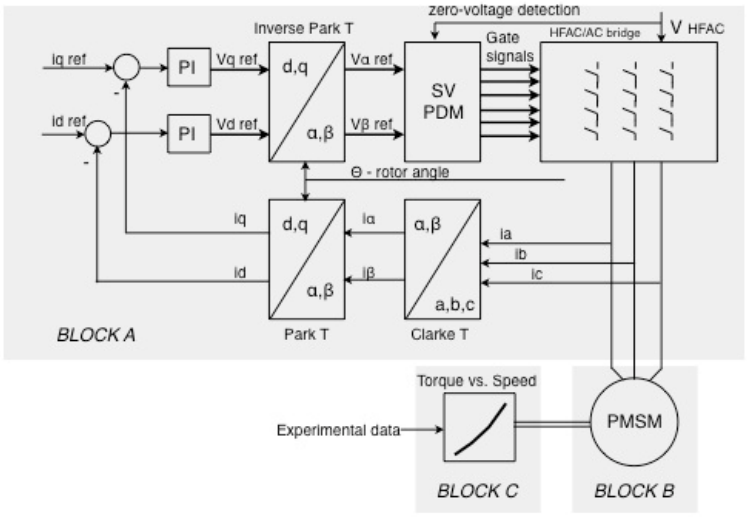

Figure 15a. Diagram of EPAS model integrating HFAC supply and SV PDM

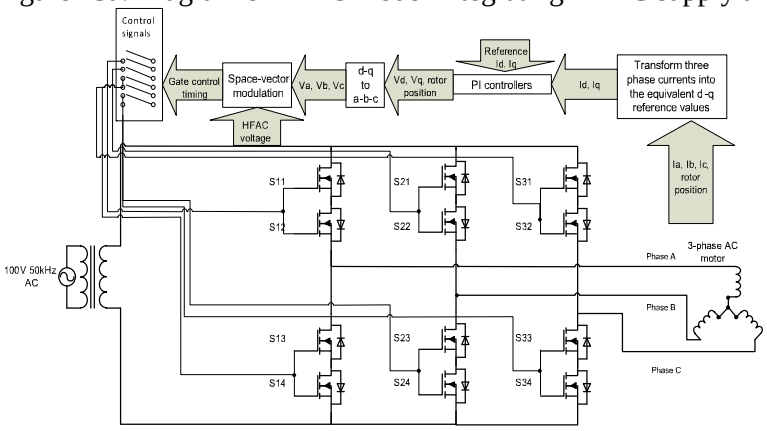

Figure 15b. Representation of the modified HFAC/AC bridge and SV PDM control

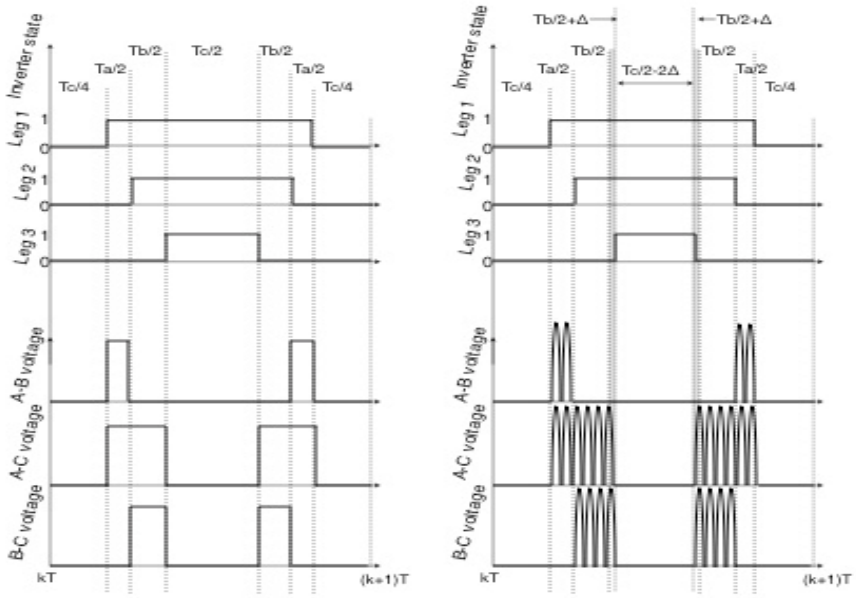

Figure 16a (left). Typical logic and associated phase-to-phase motor voltage for standard SV PWM control method
Figure 16b (right). Modified SV PDM control based on zero voltage switching

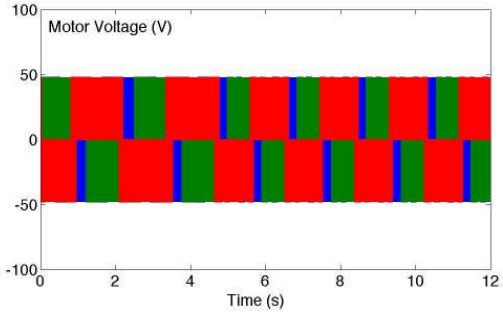

Figure 17a. DC/AC drive 3-phase voltage (V)

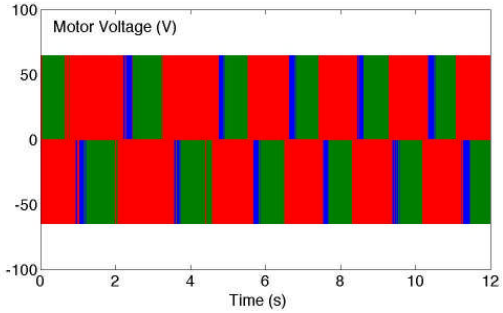

Figure 17b. HFAC/AC drive 3-phase voltage (V)

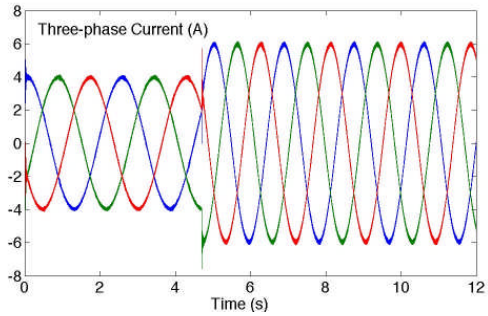

Figure 17c. DC/AC drive 3-phase current (A)

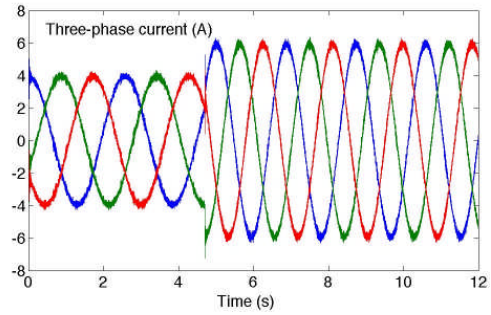

Figure 17d. HFAC/AC drive 3-phase current (A)

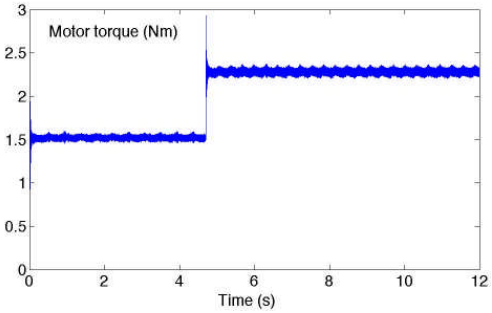

Figure 17e. DC/AC drive, PMSM torque (Nm)

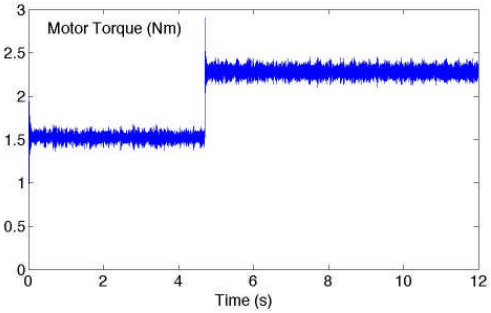

Figure 17f. HFAC/AC drive, PMSM torque (Nm)

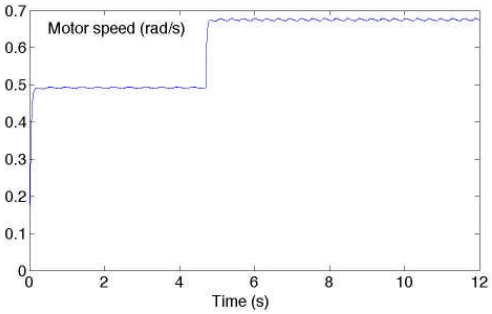

Figure 17g. DC/AC drive, PMSM speed (rad/s)

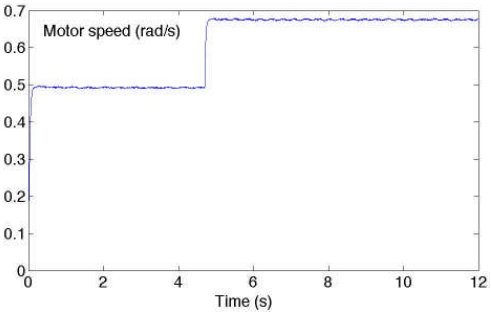

Figure 17h. HFAC/AC drive, PMSM speed (rad/s)

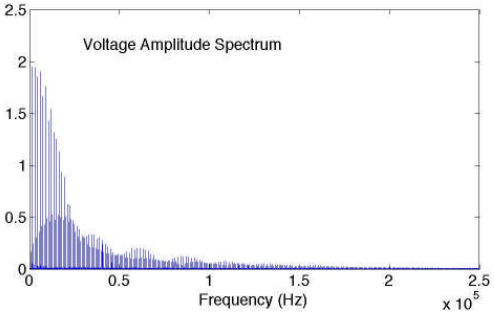

Figure 17i. DC/AC drive, voltage harmonics (relative to base value 1)

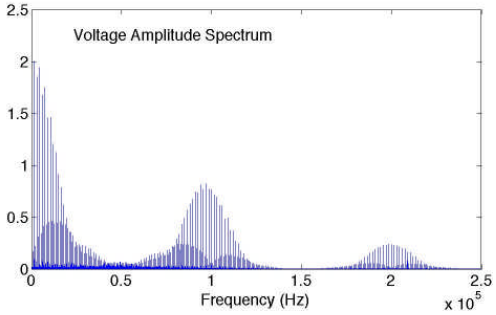

Figure 17j. HFAC/AC drive, voltage harmonics (relative to base value 1)

Figure 17. Comparison of DC/AC drive (left) and HFAC/AC drive (right) voltage, current, motor torque and speed, and voltage amplitude spectrum

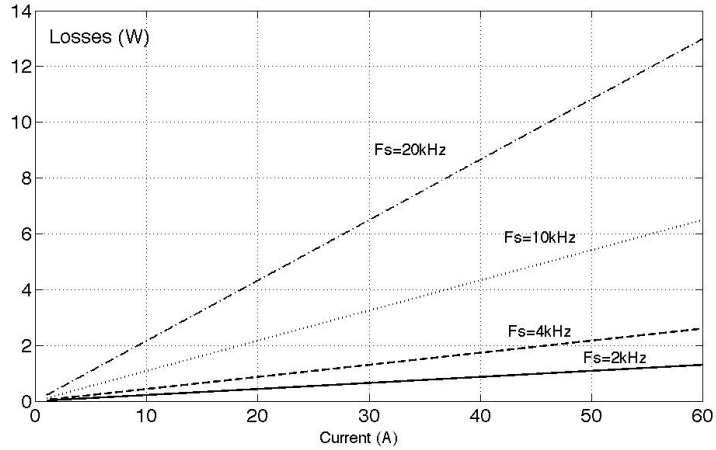

Figure 18. Switching losses associated with the operation of a DC/AC drive (W) vs. load current (A) for several switching frequencies (Fs)

TABLES

Table 1 - DC Motors

Operating Point						Dimensions			Application
Rated Power (W)	Rated Speed (rpm)	Rated Torque (Stall) (Nm)	Voltage (V)	Current (A)	Efficiency (%)	Diameter (mm)	Length (mm)	Weight (kg)	
34.5	3,360	10 (49)	12	6.8	42	52	110	0.44	Windscreen Wipers
84	4,000	20 (97)	12	12	58	59	100	0.7	Power Windows
100	3,800	20(183)	12	12	70	73	100	1.1	Radiator Fan
120	4,600	25(198)	12	15	67	73	100	1.1	Heating system, Blower
140	5,250	25(194)	12	17	69	73	100	1.1	Electric Rooftop Actuator
160	3,700	40(190)	12	18	74	73	110	1.12	Throttle Valve Actuator
181	3,450	50(400)	12	20	75	74	74	1.5	Fuel Pump

Table 2 - 400Hz AC induction motors

Operating Point						Dimensions			Possible Application
Rated Power (W)	Rated Speed (rpm)	Rated Torque (Stall) (Nm)	Voltage (V)	Current (A)	Efficiency (%)	Diameter (mm)	Length (mm)	Gear Ratio	
179	3,375	50 (84)	115	1.1	81	45	54	3.2:1	Windscreen Wipers
246	4,000	59 (95)	115	1.4	87	46	59	2.7:1	Power Windows
425	3,800	99(214)	115	2.4	88	46	75	2.9:1	Radiator Fan
647	4,600	132 (219)	115	3.3	95	46	86	2.35:1	Heating system, Blower
647	5,350	114 (188)	115	3.3	95	73	100	2:1	Electric Rooftop Actuator
425	3,700	102 (222)	115	2.4	88	46	75	3:1	Throttle Valve Actuator
725	3,367	207 (411)	115	3.7	95	66	80	3:1	Fuel Pump

Table 3. Comparison between 160W DC and 425W AC motors

Motor type	Voltage[V] (line to line rms for AC)	Nominal Power [W]	Nominal Current [A]	Nominal Speed [rpm]	Nominal Torque [Ncm]	Peak Stall torque [Ncm]	Length [mm]	Diameter [mm]	Weight [kg]
DC	12	160	18	3,700	40	190	110	73	1.12
AC	200	425W	2.41A	11,100	34	74	75.3	45.7	-
AC, with gear reduction of 3:1				3,700	102	222			

APPENDIX

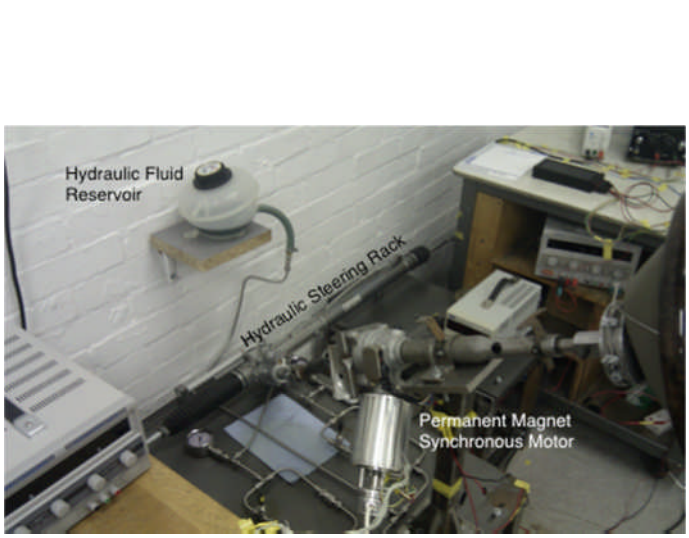

Figure A1. EPAS experimental apparatus (left)
Figure A2. Three-phase, permanent magnet synchronous motor (right)

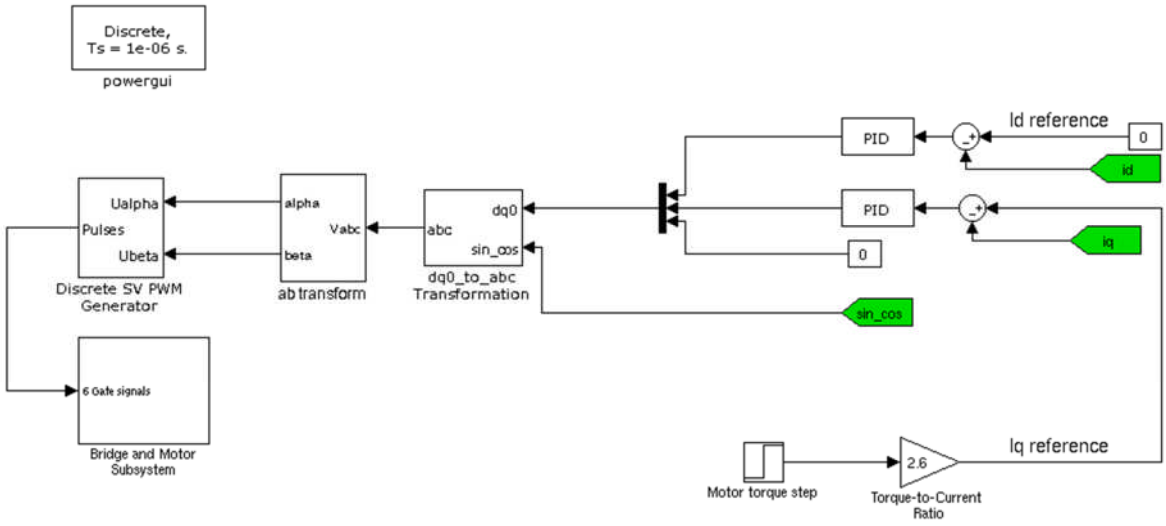

Figure A3.a Matlab Simulink model of EPAS system

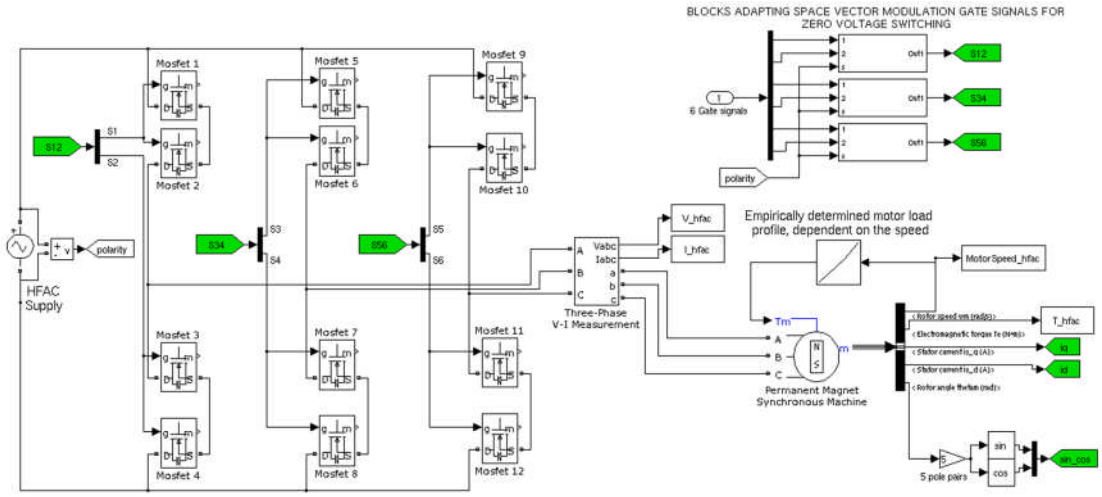

Figure A3.b HFAC/AC bridge and motor sub-system model in Matlab Simulink (corresponding to the block with the same name in the model shown in Figure A3.a)

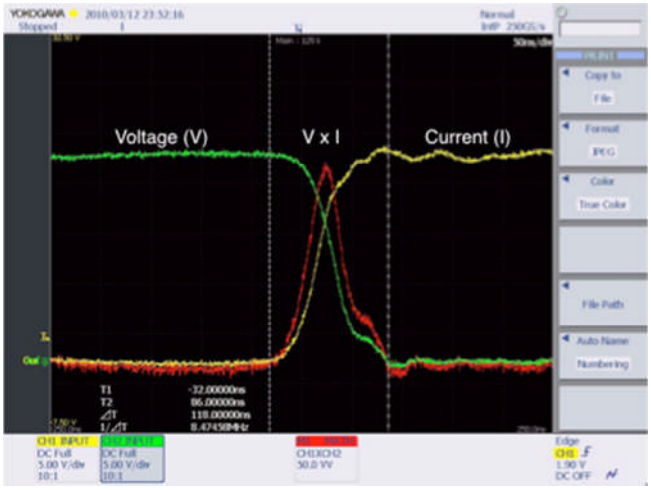

Figure A4. MOSFET turn-on: voltage, current and switching losses.
(MOSFET: IRF S4229PBF N channel, 250V, 45A, on-state resistance 0.042 ohm) (Lourdes, 2010)

Table A1. PMSM parameters

Model	12S10P
Slot number	12
Pole number	10
Rated current (A)	13.0
Rated torque (N-m)	7.03
Cogging torque, T_{cog}(N-m)	4.42e-3
T_{cog}/T_n(%)	0.063
Open-circuit voltage (V_{phase})	12.5
Iron loss (W)	3.96
Copper loss (W)	152
Efficiency (%)	73.5
Wire size (mm)	1.0
Number of turns	30
Current density (MA/m^2)	16.67
Slot fill factor (%)	55.57
Stator outer diameter (mm)	75
Stator inner diameter (mm)	41
Rotor outer diameter (mm)	40